SUPPLEMENTAL MATERIAL

SUPPLEMENTAL METHODS

Animal Studies

All animal experiments and euthanasia protocols were conducted in strict accordance with the NIH guidelines for humane treatment of animals and approved by the IACUC Committee at the Sanford-Burnham Medical Research Institute at Lake Nona. Inducible adult PGC-1$\alpha\beta^{-/-}$ mouse model (PGC-1$\alpha\beta^{-/-}$) in C57BL6/sv129 hybrid background has been previously described.[1] PGC-1$\alpha\beta$ double deficiency was induced by intraperitoneal injection of 50 mg/kg/day of tamoxifen (Sigma) dissolved in sunflower seed oil (Sigma) for 2 days, at the age of 2 months, and was compared directly with their sex-matched littermates injected with vehicle (PGC-1$\alpha^{-/-}$). Mice were harvested 1 month after injection of tamoxifen or vehicle as described below.

Mouse surgery

The transverse aortic constriction (TAC) and heart failure [combination of TAC and small apical myocardial infarction (MI)] surgeries were performed on 8-week-old female C57BL6/J mice. TAC, a surgical insult to induce compensated left ventricular hypertrophy (CH group), has been described.[2] Briefly, mice were anesthetized with ketamine [87mg/kg] / xylazine [13mg/kg]. Following aortic dissection through intercostal muscles, a 7.0 silk suture was tied around a blunt 26-28 gauge needle placed over the transverse aorta. The needle was removed to introduce a tight constriction. Combining TAC and MI surgery is a method to induce decompensated heart failure (HF group). Immediately following the TAC surgery, described above, a left thoracotomy was performed, and the left ventricle and left main coronary artery system exposed.

The left anterior descending branch (LAD) of the left coronary artery was ligated with a 9-0 nylon suture approximately ¼ distance from the apex to create a small distal MI. Four weeks post-surgery, food was removed at 0900 for 4 hours, the bi-ventricle was excised as stated below for each endpoint. Prior to analysis of all samples, the infarcted apical region was removed from the hearts of the HF mice (and the corresponding cardiac tissue region was removed from sham-operated controls). 2-3 hearts per sample were pulverized, pooled, and split for transcriptomic and metabolomic analysis.

Echocardiography

Echocardiography was performed non-invasively using a Vevo 2100 microultrasound System (VisualSonics Inc, Toronto, Ontario, Canada) as described.[3,4] Briefly, adult mice were anesthetized with an intraperitoneal injection (0.05 mg/g) of 2% avertin (to maintain heart rate close to 600 beats per minute or above in order to evaluate left ventricular systolic function) which was followed by continuous inhalation of 1-1.5% gaseous isoflurane administered through a customized nose cone for detailed cardiac morphometric analysis. Complete 2D and Doppler ultrasound examinations were performed using multiple views. The following cardiac function parameters were collected: heart rate (HR), end diastolic volume (EDV), end systolic volume (ESV), ejection fraction (EF), and velocity time integral (VTI) ratio, a ratio of blood flow velocity at the TAC constriction band site to that at the left ventricular outflow tract, used to confirm significant aortic constriction.

Exercise training

Mice were exercise-trained following a modified version of the voluntary running-wheel

protocol described previously.[5] Two-month-old female C57BL/6 mice were housed for two months in individual cages equipped with 4.5" diameter Run-Around exercise wheels (Super Pet, Elk Grove village, IL). The daily running distances were recorded and monitored via a Bell F12 cyclocomputer (Easton-Bell Sports, Van Nuys, CA). Mice that did not run at least 5 miles per night were removed from the study. Twenty-four hours after removing the exercise wheels, food was removed at 0900 for 4 hours, the bi-ventricle was excised, rinsed in PBS, and freeze-clamped in liquid nitrogen. 2-3 hearts per sample were pulverized, pooled, and split for transcriptomic and metabolomic analysis.

RNA analysis and RT-PCR

Total RNA was isolated from mouse bi-ventricle using the RNAzol method (Tel-Test). Quantitative real-time RT-PCR was performed as previously described.[6] In brief, total RNA was isolated and reverse transcribed with AffinityScript QPCR cDNA Synthesis Kit (Ailgent Technologies). PCR reactions were performed in triplicate in a 96-well format using a MX3005P Real-Time PCR System (Stratagene). The mouse-specific primer sets (SYBR green) used to detect specific gene expression can be found in Supplemental Table 1. 36B4 primer set was included in a separate well (in triplicate) and used to normalize the gene expression data.

Immunoblotting studies

Western blotting was performed with bi-ventricle protein lysates as previously described.[7] The following antibodies were used: Rabbit polyclonal MCAD antibody;[8] Rabbit polyclonal LCAD and VLCAD antibodies (provided by Arnold W. Strauss, University of Cincinnati College of Medicine) as previously described;[9,10] Ribosomal protein s6 (S6RP) (Cell Signaling Technology

No. 2217S). Detection was performed by measuring the chemiluminescent signal as assayed by SuperSignal Dura (Pierce).

Mitochondrial respiration

Mitochondrial respiration rates were determined on saponin-permeabilized left ventricular muscle strips with palmitoylcarnitine (20μM)/malate (5mM) and pyruvate (10mM)/malate (5mM) as substrate as previously described.[11] In brief, 3 month-old female C57BL/6 mice (one month post-surgery) were euthanized by CO_2 inhalation. The muscle fibers from left ventricular myocardium were separated and then transferred to a buffer (2.77 mM K_2Ca-EGTA, 7.23 mM K_2EGTA, 6.56 mM $MgCl_2$, 20 mM imidazole, 53.3 mM K-MES, 20 mM taurine, 5.3 mM ATP, 15 mM PCr, 3 mM KH_2PO4, 0.5 mM DTT [pH 7.1]) supplemented with 50 μg/ml saponin and permeabilized for 30 min at 4°C with gentle stirring. Fibers were then washed twice for 10 min each (2.77 mM K_2Ca-EGTA, 7.23 mM K_2EGTA, 1.38 mM $MgCl_2$, 20 mM imidazole, 100 mM K-MES, 20 mM taurine, 3 mM KH_2PO4, 0.5 mM DTT, 2 mg/ml BSA [pH 7.1]). Mitochondrial respiration was performed at 25°C using an optical probe (Oxygen FOXY Probe, Ocean Optics). Following measurement of basal respiration, maximal (ADP-stimulated) respiration was determined by exposing the mitochondria to 1 mM ADP. Uncoupled respiration was evaluated following addition of oligomycin (1 μg/mL). The solubility of oxygen in the respiration buffer at 25°C was taken as 230 nmol O_2 per milliliter. Respiration rates were expressed as "nmol O_2 min^{-1} mg dry $weight^{-1}$".

Gene Microarray and Pathway Analysis

To conduct transcriptomimcs analysis in mouse heart, immediately following deep anesthesia by

intraperitoneal injection of pentobarbital (100mg/kg body weight), bi-ventricle was excised, rinsed in PBS, and freeze-clamped in liquid nitrogen. Total RNA was isolated from powdered bi-ventricle using the RNAzol method (Tel-Test). The Analytical Genomics Core at Sanford-Burnham Medical Research Institute performed gene microarray studies by using Affymetrix GeneChip Mouse Gene 1.0 ST array. The Affymetrix probe level data was processed using Robust Multi-Array Analysis (RMA) to obtain normalized summary scores of expression for each probe set on each array.[12] EBarrays was used to identify genes differentially expressed in any two conditions,[13,14] including CH vs sham, HF vs sham, Run (PH) vs Sedentary. R was used for both RMA and EBarrays analysis. The list of genes with posterior probabilities greater than or equal to 0.95 (expected FDR less than 5%) was considered a regulated gene. Linear regression analysis (Igor Pro, Wavemetrics) was used to assess the correlation between the fold change in gene expression between CH and HF models. All genes in the canonical pathways of Fatty Acid Metabolism, Tricarboxylic Acid (TCA) Cycle, and Oxidative Phosphorylation defined by Ingenuity Pathway Analysis (IPA; version #11631407) were used to create the heat map. The heat map for transcriptomics was generated by using the log2-transformed fold change of average expression in experimental group vs control, including CH vs sham, HF vs sham, Run (PH) vs Sedentary, and PGC-1$\alpha\beta^{-/-}$ vs. PGC-1$\alpha^{-/-}$ control. The gene array data discussed in this publication have been deposited in NCBI's Gene Expression Omnibus and are accessible through GEO Series accession number GSE56348. The following link has been created to allow review of record GSE56348 prior to publication:
http://www.ncbi.nlm.nih.gov/geo/query/acc.cgi?token=mxavguwebfaptcp&acc=GSE56348

For pathway analysis, either upregulated or downregulated genes were uploaded into Ingenuity Pathway Analysis (IPA) software. The core analysis was used to interpret data, and the

pathways were reviewed using the canonical pathways defined by IPA (Version #17199142). The p value was calculated using Fisher's exact test. The pathways with a p value less than 0.05 were considered a regulated pathway. Canonical pathways were grouped into the function category defined by IPA, which is ranked by the total number of pathways regulated in the category. To map the genes regulated in canonical pathways defined by IPA, the genes with posterior probabilities greater than or equal to 0.95 were uploaded into IPA, and the genes in the biopathway as well as the directionality of regulation were reviewed.

Metabolomics

To conduct metabolomics analysis in mouse heart, immediately following deep anesthesia by intraperitoneal injection of pentobarbital (100mg/kg body weight), bi-ventricle was excised, rinsed in PBS, and freeze-clamped in liquid nitrogen. Specimens of powdered bi-ventricle tissue were diluted 20-fold (mass:volume) in 50% acetonitrile supplemented with 0.3% formate (acylcarnitines, amino acids, and organic acids). Samples were homogenized in a TissueLyser II (Qiagen). Tissue extracts were derivatized and analyzed as previously described.[15] Levels of amino acids, acylcarnitines, and organic acids were determined using stable isotope dilution techniques. Amino acid and acylcarnitine measurements prepared from tissue homogenate and plasma were made using flow injection tandem mass spectrometry using sample preparation methods described previously.[16,17] The data were acquired using a Waters Acquity™ UPLC system equipped with a TQ (triple quadrupole) detector and a data system controlled by MassLynx 4.1 operating system (Waters, Milford, MA). Organic acids were quantified using methods described previously,[18] employing Trace Ultra GC coupled to a Trace DSQ MS operating under Excalibur 1.4 (Thermo Fisher Scientific, Austin, TX). The heat map for

metabolomics was generated using the log2-transformed fold change of average value of metabolites in experimental group vs control, including CH vs sham, HF vs sham, Run (PH) vs Sedentary, and PGC-1$\alpha\beta^{-/-}$ vs. PGC-1$\alpha^{-/-}$ control.

Supplemental Table 1. Mouse primer sequences for qRT-PCR analysis.

Primers	Forward	Reverse
Slc27a1	ATCTACGGGTTGACGGTGGTA	GGTAGCGGCAGATTTCACCTA
Cpt1b	ATGTCTACCTCCGAAGCAGGA	GCTGCTTGCACATTTGTGTTC
Cpt2	GCACAGAAGCCTCTCTTGAATG	TCTGTTTATCCTGAGCGAGCA
Acadvl	ATCTCTGCCCAGCGACTTT	TTCTGGCTTGTCCAGAACTG
Ehhadh	GCCATAGTGATCTGTGGAGCA	CCACCACTGGCTTCTGGTATC
36B4	TGGAAGTCCAACTACTTCCTCAA	ATCTGCTGCATCTGCTTGGAG

Supplemental Table 2. Echocardiographic analysis of HF mice.

Parameters	Sham (HF)	HF	p-value
N	5	23-24	
HR (bpm)	615.0 ± 14.5	608.0 ± 36.84	0.44
EF (%)	69.51 ± 3.63	38.42 ± 12.78*	<0.001
EDV (ul)	27.14 ± 6.08	59.69 ± 16.07*	<0.001
ESV (ul)	8.35 ± 2.62	38.32 ± 17.10*	<0.001
VTI ratio	0.63 ± 0.12	5.89 ± 1.71*	<0.001

*$p < 0.05$ compared with sham (HF). HR, Heart rate; EF, Ejection fraction; EDV, End diastolic volume; ESV, End systolic volume; VTI ratio, Velocity time integral ratio.

Supplemental Table 3. Pathways containing upregulated or downregulated genes in CH myocardium.

Pathway/Function Categories	Pathways	# of genes regulated	# of genes in pathway	p-Value
Downregulated				
Lipid Metabolism	LPS/IL-1 Mediated Inhibition of RXR Function	12	215	<0.001
	PXR/RXR Activation	6	60	<0.001
	Glutaryl-CoA Degradation	3	11	<0.001
	AMPK Signaling	7	134	0.006
	Noradrenaline and Adrenaline Degradation	3	29	0.012
	Fatty Acid β-oxidation I	3	30	0.013
	Ubiquinol-10 Biosynthesis (Eukaryotic)	2	12	0.014
	Glutathione Redox Reactions I	2	16	0.026
AA Metabolism	Valine Degradation I	4	18	<0.001
	Isoleucine Degradation I	3	14	0.002
	Branched-chain α-keto acid Dehydrogenase Complex	2	4	0.002
	Tryptophan Degradation X (Mammalian, via Tryptamine)	2	17	0.030
	Putrescine Degradation III	2	16	0.030
	Dopamine-DARPP32 Feedback in cAMP Signaling	6	155	0.046
Cell Signaling	G-Protein Coupled Receptor Signaling	11	253	0.004
	Cellular Effects of Sildenafil (Viagra)	7	123	0.005
	cAMP-mediated signaling	9	211	0.010
	Aryl Hydrocarbon Receptor Signaling	6	139	0.023
Carbohydrate Metabolism	Glutathione-mediated Detoxification	6	23	<0.001
	tRNA Splicing	3	34	0.020
Lipid and AA Metabolism	Tryptophan Degradation III (Eukaryotic)	3	20	0.004
	Phenylalanine Degradation IV (Mammalian, via Side Chain)	2	13	0.020
Growth and Development	HIF1α Signaling	5	101	0.026
Other	Xenobiotic Metabolism Signaling	12	264	<0.001
	Myo-inositol Biosynthesis	2	4	0.002
	Serotonin Degradation	3	47	0.031
	D-myo-inositol (1,4,5)-trisphosphate Degradation	2	18	0.037
	Dopamine Degradation	2	20	0.042
Upregulated				
Immune/Inflammatory Response	IL-8 Signaling	13	183	0.014
	HMGB1 Signaling	8	92	0.019
	iNOS Signaling	5	45	0.021
	Regulation of IL-2 Expression in Activated and Anergic T Lymphocytes	7	82	0.021
	Interferon Signaling	4	29	0.021
	MIF-mediated Glucocorticoid Regulation	4	33	0.027
	Chemokine Signaling	6	66	0.033
	TREM1 Signaling	5	54	0.037
	Toll-like Receptor Signaling	5	53	0.037
	Prostanoid Biosynthesis	2	9	0.042
	CXCR4 Signaling	10	152	0.046
	CCR3 Signaling in Eosinophils	8	114	0.048
Growth and Development	TGF-β Signaling	9	84	0.003
	Role of NFAT in Cardiac Hypertrophy	14	182	0.004
	VEGF Signaling	9	94	0.005
	Cardiac Hypertrophy Signaling	16	219	0.005
	Colorectal Cancer Metastasis Signaling	16	237	0.010
	Glucocorticoid Receptor Signaling	16	264	0.022
	Cardiomyocyte Differentiation via BMP Receptors	3	19	0.023
	Melanocyte Development and Pigmentation Signaling	7	83	0.031
	Neuregulin Signaling	7	93	0.032
	Pancreatic Adenocarcinoma Signaling	8	111	0.042
Cell Signaling	RhoA Signaling	11	114	0.003
	Gap Junction Signaling	12	152	0.009
	Sphingosine-1-phosphate Signaling	9	109	0.014
	Synaptic Long Term Depression	10	142	0.026

	Role of Macrophages, Fibroblasts and Endothelial Cells in Rheumatoid Arthritis	17	300	0.030
	α-Adrenergic Signaling	7	87	0.032
	G Beta Gamma Signaling	7	97	0.038
	D-myo-inositol-5-phosphate Metabolism	9	132	0.043
Cellular Assembly and Organization	Remodeling of Epithelial Adherens Junctions	8	65	0.002
	Epithelial Adherens Junction Signaling	12	142	0.005
	Actin Nucleation by ARP-WASP Complex	6	64	0.016
	Integrin Signaling	13	202	0.026
	Axonal Guidance Signaling	23	440	0.034
	Semaphorin Signaling in Neurons	5	51	0.040
	Germ Cell-Sertoli Cell Junction Signaling	10	154	0.049
Cellular Movement	Hepatic Fibrosis / Hepatic Stellate Cell Activation	21	137	<0.001
	Macropinocytosis Signaling	7	73	0.012
	Virus Entry via Endocytic Pathways	8	88	0.013
	Inhibition of Matrix Metalloproteases	4	37	0.047
Lipid Metabolism	PPARα/RXRα Activation	11	173	0.041
Other	Endothelin-1 Signaling	14	167	0.003
	eNOS Signaling	10	127	0.014
	Role of Osteoblasts, Osteoclasts and Chondrocytes in Rheumatoid Arthritis	14	219	0.027
	Apoptosis Signaling	7	89	0.032
	Systemic Lupus Erythematosus Signaling	11	190	0.038
	UDP-N-acetyl-D-galactosamine Biosynthesis I	2	9	0.042

The p value was calculated by Fisher's exact test. $p<0.05$ was considered statistically significant.

Supplemental Table 4. Pathways containing upregulated or downregulated genes in HF myocardium.

Pathway/Function Category	Pathways	# of genes regulated	# of genes in pathway	p-Value
Downregulated				
Lipid Metabolism	Fatty Acid β-oxidation I	8	30	<0.001
	LPS/IL-1 Mediated Inhibition of RXR Function	20	215	<0.001
	AMPK Signaling	14	134	<0.001
	Glutaryl-CoA Degradation	4	11	<0.001
	Oxidative Ethanol Degradation III	4	28	0.001
	Mitochondrial L-carnitine Shuttle Pathway	4	18	0.002
	Ethanol Degradation II	5	28	0.002
	Ethanol Degradation IV	4	18	0.002
	Noradrenaline and Adrenaline Degradation	5	29	0.002
	Fatty Acid β-oxidation III (Unsaturated, Odd Number)	2	3	0.003
	Stearate Biosynthesis I (Animals)	5	34	0.005
	Fatty Acid α-oxidation	3	14	0.009
	PXR/RXR Activation	6	60	0.011
	Glutathione Redox Reactions I	3	16	0.013
	Triacylglycerol Degradation	3	23	0.042
AA Metabolism	Tryptophan Degradation X (Mammalian, via Tryptamine)	4	17	0.002
	Putrescine Degradation III	4	16	0.002
	Leucine Degradation I	3	9	0.003
	TR/RXR Activation	8	85	0.006
	Branched-chain α-keto acid Dehydrogenase Complex	2	4	0.007
	Valine Degradation I	3	18	0.021
Immune/Inflammatory Response	IL-22 Signaling	4	24	0.008
	Role of JAK2 in Hormone-like Cytokine Signaling	4	34	0.022
	IL-9 Signaling	4	35	0.027
	IL-3 Signaling	6	71	0.029
	IL-2 Signaling	5	55	0.033
Carbohydrate Metabolism	Glutathione-mediated Detoxification	5	23	0.001
	Type II Diabetes Mellitus Signaling	10	127	0.005
	Glycolysis I	3	22	0.037
	Gluconeogenesis I	3	23	0.042
Cell Signaling	Aryl Hydrocarbon Receptor Signaling	11	139	0.004
	RAR Activation	13	172	0.004
	G-Protein Coupled Receptor Signaling	14	253	0.043
Growth and Development	Growth Hormone Signaling	7	69	0.007
	FGF Signaling	7	86	0.023
	Thrombopoietin Signaling	5	58	0.035
Lipid and AA Metabolism	Proline Degradation	2	2	0.001
	Tryptophan Degradation III (Eukaryotic)	4	20	0.003
Carbohydrate and AA Metabolism	Alanine Degradation III	2	2	0.001
	Alanine Biosynthesis II	2	2	0.001
Lipid and Carbohydrate Metabolism	Acyl-CoA Hydrolysis	3	11	0.005
Cellular Assembly and Orgnization	GDNF Family Ligand-Receptor Interactions	6	69	0.028
Other	Xenobiotic Metabolism Signaling	20	264	<0.001
	Dopamine Degradation	4	20	0.003
	NRF2-mediated Oxidative Stress Response	13	182	0.005
	Myo-inositol Biosynthesis	2	4	0.007
	Histamine Degradation	3	13	0.009
	Serotonin Degradation	5	47	0.011
Upregulated				
Immune/Inflammatory Response	IL-8 Signaling	23	183	<0.001
	TREM1 Signaling	11	54	<0.001
	Acute Phase Response Signaling	20	163	<0.001
	Leukocyte Extravasation Signaling	22	193	<0.001
	Dendritic Cell Maturation	18	172	0.001
	Macropinocytosis Signaling	11	73	0.001
	Agranulocyte Adhesion and Diapedesis	19	166	0.001
	Role of Pattern Recognition Receptors in Recognition of Bacteria and Viruses	13	95	0.001

	Granulocyte Adhesion and Diapedesis	16	155	0.005
	Fcγ Receptor-mediated Phagocytosis in Macrophages and Monocytes	11	94	0.007
	Prostanoid Biosynthesis	3	9	0.009
	Altered T Cell and B Cell Signaling in Rheumatoid Arthritis	9	84	0.012
	T Helper Cell Differentiation	8	68	0.012
	HMGB1 Signaling	10	92	0.018
	Natural Killer Cell Signaling	10	95	0.021
	IL-17 Signaling	8	68	0.021
	NF-κB Activation by Viruses	8	76	0.029
	IL-6 Signaling	11	116	0.030
	Antiproliferative Role of TOB in T Cell Signaling	4	26	0.037
	NF-κB Signaling	13	161	0.041
	Role of IL-17F in Allergic Inflammatory Airway Diseases	5	42	0.044
Growth and Development	ILK Signaling	24	178	<0.001
	Colorectal Cancer Metastasis Signaling	27	237	<0.001
	VEGF Signaling	14	94	<0.001
	Factors Promoting Cardiogenesis in Vertebrates	13	88	<0.001
	Ovarian Cancer Signaling	16	134	0.001
	Pancreatic Adenocarcinoma Signaling	14	111	0.001
	Wnt/β-catenin Signaling	18	168	0.002
	TGF-β Signaling	11	84	0.003
	Neuregulin Signaling	11	93	0.003
	HGF Signaling	12	101	0.004
	Human Embryonic Stem Cell Pluripotency	14	142	0.006
	Role of NFAT in Cardiac Hypertrophy	17	182	0.006
	Melanocyte Development and Pigmentation Signaling	10	83	0.008
	IGF-1 Signaling	11	98	0.009
	Bladder Cancer Signaling	10	88	0.011
	HIF1α Signaling	11	101	0.012
	HER-2 Signaling in Breast Cancer	9	77	0.012
	Chronic Myeloid Leukemia Signaling	10	98	0.018
	Cardiac Hypertrophy Signaling	18	219	0.024
	Molecular Mechanisms of Cancer	25	347	0.028
	VEGF Family Ligand-Receptor Interactions	8	74	0.031
	Salvage Pathways of Pyrimidine Ribonucleotides	8	80	0.049
Cell Signaling	Role of Macrophages, Fibroblasts and Endothelial Cells in Rheumatoid Arthritis	35	300	<0.001
	RhoA Signaling	13	114	0.005
	Signaling by Rho Family GTPases	21	239	0.006
	Aryl Hydrocarbon Receptor Signaling	14	139	0.006
	Sphingosine-1-phosphate Signaling	12	109	0.006
	Caveolar-mediated Endocytosis Signaling	9	78	0.009
	Rac Signaling	11	112	0.014
	Gα12/13 Signaling	12	118	0.015
	p38 MAPK Signaling	11	111	0.023
	RhoGDI Signaling	15	184	0.028
	PI3K/AKT Signaling	11	131	0.038
	Gap Junction Signaling	13	152	0.039
	Docosahexaenoic Acid (DHA) Signaling	5	39	0.039
	Phospholipase C Signaling	17	232	0.048
Cellular Assembly and Organization	Epithelial Adherens Junction Signaling	20	142	<0.001
	Axonal Guidance Signaling	40	440	<0.001
	Clathrin-mediated Endocytosis Signaling	21	180	<0.001
	Actin Cytoskeleton Signaling	21	222	0.002
	Remodeling of Epithelial Adherens Junctions	9	65	0.005
	Integrin Signaling	18	202	0.010
	Paxillin Signaling	11	108	0.012
	Ephrin Receptor Signaling	16	188	0.013
	Germ Cell-Sertoli Cell Junction Signaling	14	154	0.020
	Semaphorin Signaling in Neurons	6	51	0.046
Cellular Movement	Hepatic Fibrosis / Hepatic Stellate Cell Activation	34	137	<0.001
	Inhibition of Matrix Metalloproteases	8	37	<0.001
	Atherosclerosis Signaling	14	117	0.001
	Glioma Invasiveness Signaling	9	57	0.002
	Role of Tissue Factor in Cancer	13	110	0.003
	Virus Entry via Endocytic Pathways	11	88	0.004
	Regulation of the Epithelial-Mesenchymal Transition Pathway	17	185	0.010

	Oncostatin M Signaling	5	33	0.025
Lipid Metabolism	LXR/RXR Activation	11	114	0.024
	Fatty Acid α-oxidation	3	14	0.026
	Eicosanoid Signaling	7	60	0.033
	Hepatic Cholestasis	12	135	0.033
	PPARα/RXRα Activation	14	173	0.041
AA Metabolism	Proline Biosynthesis I	2	4	0.015
	Tryptophan Degradation X (Mammalian, via Tryptamine)	3	17	0.046
	Putrescine Degradation III	3	16	0.046
Other	Role of Osteoblasts, Osteoclasts and Chondrocytes in Rheumatoid Arthritis	27	219	<0.001
	eNOS Signaling	14	127	0.004
	Amyotrophic Lateral Sclerosis Signaling	11	97	0.009
	Intrinsic Prothrombin Activation Pathway	5	32	0.009
	Dopamine Degradation	4	20	0.014
	Endothelin-1 Signaling	15	167	0.020
	Inhibition of Angiogenesis by TSP1	5	33	0.022
	Tetrahydrofolate Salvage from 5,10-methenyltetrahydrofolate	2	5	0.024
	Coagulation System	5	35	0.028
	Superoxide Radicals Degradation	2	6	0.035

The p value was calculated by Fisher's exact test. $p<0.05$ was considered statistically significant.

Supplemental Table 5. Differentially expressed genes involved in fatty acid metabolism in CH and HF model.

Symbol	Gene Name	CH		HF	
		FC	DE	FC	DE
Aldh1a1	aldehyde dehydrogenase family 1, subfamily A1	1.470	**1.000**	1.587	**1.000**
Gcdh	glutaryl-Coenzyme A dehydrogenase	-1.385	**0.999**	-1.361	**1.000**
Slc27a1	solute carrier family 27 (fatty acid transporter), member 1	-1.443	**0.999**	-1.490	**1.000**
Eci1	enoyl-Coenzyme A delta isomerase 1	-1.289	0.557	-1.357	**1.000**
Acaa2	acetyl-Coenzyme A acyltransferase 2	-1.335	0.545	-1.404	**1.000**
Adhfe1	alcohol dehydrogenase, iron containing, 1	-1.274	0.104	-1.427	**1.000**
Aldh4a1	aldehyde dehydrogenase 4 family, member A1	-1.256	0.535	-1.335	**1.000**
Aldh2	aldehyde dehydrogenase 2, mitochondrial	-1.307	**0.985**	-1.418	**1.000**
Ech1	enoyl coenzyme A hydratase 1, peroxisomal	-1.366	0.674	-1.458	**1.000**
Ehhadh	enoyl-Coenzyme A, hydratase/3-hydroxyacyl Coenzyme A dehydrogenase	-1.486	**0.984**	-1.908	**1.000**
Aldh9a1	aldehyde dehydrogenase 9, subfamily A1	-1.205	0.050	-1.361	**1.000**
Aldh1a2	aldehyde dehydrogenase family 1, subfamily A2	1.292	0.209	1.319	**0.999**
Acadvl	acyl-Coenzyme A dehydrogenase, very long chain	-1.232	0.106	-1.267	**0.998**
Cpt2	carnitine palmitoyltransferase 2	-1.297	0.827	-1.321	**0.998**
Cpt1a	carnitine palmitoyltransferase 1a, liver	-1.202	0.328	-1.348	**0.998**
Acsl5	acyl-CoA synthetase long-chain family member 5	1.238	0.319	1.257	**0.996**
Hadh	hydroxyacyl-Coenzyme A dehydrogenase	-1.220	0.040	-1.264	**0.994**
Acsl6	acyl-CoA synthetase long-chain family member 6	-1.195	0.536	-1.242	**0.953**
Hsd17b10	hydroxysteroid (17-beta) dehydrogenase 10	-1.309	**1.000**	-1.235	0.937

FC, fold change; DE, posterior probability of differential expression; genes with DE ≥ 0.950 (bolded) are significantly regulated.

Supplemental Table 6. Differentially expressed genes involved in amino acid degradation pathways in CH and HF.

Symbol	Gene Name	AA Degradation Pathway	CH		HF	
			FC	DE	FC	DE
Acaa2	acetyl-Coenzyme A acyltransferase 2	Ile	-1.335	0.545	-1.404	**1.000**
Aldh2	aldehyde dehydrogenase 2, mitochondrial	Trp, Phe	-1.307	**0.985**	-1.418	**1.000**
Aldh4a1	aldehyde dehydrogenase 4 family, member A1	Pro, Trp	-1.256	0.535	-1.335	**1.000**
Aldh9a1	aldehyde dehydrogenase 9, subfamily A1	Trp, Phe	-1.205	0.050	-1.361	**1.000**
Bckdhb	branched chain ketoacid dehydrogenase E1, beta polypeptide	Val, Leu, Ile	-1.357	**0.988**	-1.458	**1.000**
Ech1	enoyl coenzyme A hydratase 1, peroxisomal	Val, Leu, Ile	-1.366	0.674	-1.458	**1.000**
Ehhadh	enoyl-Coenzyme A, hydratase/3-hydroxyacyl Coenzyme A dehydrogenase	Trp, Val, Leu, Ile	-1.486	**0.984**	-1.908	**1.000**
Gcdh	glutaryl-Coenzyme A dehydrogenase	Trp	-1.385	**0.999**	-1.361	**1.000**
Gpt	glutamic pyruvic transaminase, soluble	Ala	-1.247	0.818	-1.408	**1.000**
Gpt2	glutamic pyruvate transaminase (alanine aminotransferase) 2	Ala	-1.495	**0.999**	-1.592	**1.000**
Maob	monoamine oxidase B	Trp, Phe	-1.484	**0.994**	-1.631	**1.000**
Mccc1	methylcrotonoyl-Coenzyme A carboxylase 1 (alpha)	Leu	-1.255	0.705	-1.309	**1.000**
Mccc2	methylcrotonoyl-Coenzyme A carboxylase 2 (beta)	Leu	-1.285	0.871	-1.300	**1.000**
Prodh	proline dehydrogenase	Pro	-1.250	0.397	-1.351	**1.000**
Aldh1a1	aldehyde dehydrogenase 1 family, member A1	Val, Trp	1.470	**1.000**	1.587	**1.000**
Bckdha	branched chain ketoacid dehydrogenase E1, alpha polypeptide	Val, Leu, Ile	-1.309	**0.970**	-1.311	**0.999**
Ivd	isovaleryl coenzyme A dehydrogenase	Leu	-1.230	0.021	-1.319	**0.999**
Aldh1a2	aldehyde dehydrogenase 1 family, member A2	Val, Trp	1.292	0.209	1.319	**0.999**
Abat	4-aminobutyrate aminotransferase	Val	1.317	0.937	1.329	**0.999**
Acadvl	acyl-Coenzyme A dehydrogenase, very long chain	Val, Leu, Ile	-1.232	0.106	-1.267	**0.998**
Hadh	hydroxyacyl-Coenzyme A dehydrogenase	Ile, Trp	-1.220	0.040	-1.264	**0.994**
H2-Ke6	H2-K region expressed gene 6	Trp	-1.114	0.011	-1.220	**0.990**
Maoa	monoamine oxidase A	Trp, Phe	1.222	0.872	1.276	**0.976**
Pcca	propionyl-Coenzyme A carboxylase, alpha polypeptide	Val, Ile	-1.133	0.014	-1.209	**0.975**
Hsd17b10	hydroxysteroid (17-beta) dehydrogenase 10	Trp, Ile	-1.309	**1.000**	-1.235	0.937
Bcat2	branched chain aminotransferase 2, mitochondrial	Val, Ile	-1.302	**1.000**	-1.225	0.838
Kmo	kynurenine 3-monooxygenase (kynurenine 3-hydroxylase)	Trp	1.248	**0.957**	1.139	0.032

FC, fold change; DE, posterior probability of differential expression; genes with DE≥ 0.950 (bolded) are significantly regulated.

Supplemental Table 7. Metabolite measurements from CH, HF, and PH hearts.

Metabolites	Sham-CH (n=6)	CH (n=6)	Sham-HF (n=6)	HF (n=6)	Sed (n=6)	PH (Run) (n=6)
Acylcarnitine						
C0	1076.580±97.603	957.148±118.173*	985.941±77.057	727.739±91.744*	1116.819±77.572	1075.371±96.877
C2	116.975±9.806	130.096±33.841	150.543±18.575	219.455±32.981*	136.486±22.294	118.301±24.004
C3	5.005±0.775	3.761±0.498*	6.552±0.418	5.008±0.826*	5.736±0.560	4.513±0.611*
C4/Ci4	1.562±0.507	1.291±0.278	1.904±0.351	2.522±0.868	1.167±0.353	1.278±0.757
C5:1	1.985±0.207	1.979±0.230	1.794±0.317	1.982±0.281	1.372±0.177	1.102±0.171*
C5	0.810±0.170	1.007±0.163	0.826±0.144	1.101±0.420	0.595±0.124	0.656±0.191
C4-OH	2.699±0.459	2.751±1.020	3.648±0.557	7.705±3.270*	2.419±0.875	1.236±0.588*
C6	0.303±0.070	0.314±0.087	0.372±0.070	0.558±0.160*	0.216±0.050	0.156±0.060
C5-OH	2.403±0.378	2.920±0.371*	2.181±0.276	2.295±0.537	1.758±0.144	2.173±0.472
C3-DC	3.267±0.275	2.912±0.310	3.024±0.276	2.542±0.216*	2.511±0.187	2.154±0.318
C4-DC/Ci4-DC	10.255±0.991	5.652±1.590*	8.968±0.560	4.194±0.142*	6.699±0.617	5.939±0.689
C8:1	0.425±0.105	0.378±0.055	0.330±0.065	0.344±0.078	0.175±0.040	0.131±0.038
C8	0.188±0.032	0.163±0.026	0.213±0.064	0.232±0.071	0.105±0.017	0.103±0.036
C5-DC	0.144±0.080	0.142±0.014	0.227±0.082	0.125±0.020*	0.096±0.041	0.102±0.013
C8:1-OH/C6:1-DC	0.089±0.040	0.117±0.020	0.085±0.034	0.127±0.048	0.096±0.022	0.071±0.027
C6-DC/C8-OH	0.191±0.052	0.212±0.064	0.173±0.028	0.316±0.086*	0.252±0.067	0.150±0.031*
C10:3	0.285±0.070	0.276±0.040	0.238±0.032	0.254±0.041	0.063±0.020	0.051±0.011
C10:2	0.046±0.009	0.054±0.015	0.054±0.030	0.044±0.016	0.030±0.023	0.019±0.007
C10:1	0.137±0.033	0.113±0.032	0.145±0.035	0.136±0.043	0.096±0.029	0.069±0.023
C10	0.229±0.038	0.178±0.073	0.262±0.096	0.313±0.106	0.138±0.033	0.117±0.048
C7-DC	0.037±0.018	0.027±0.008	0.039±0.017	0.040±0.024	0.051±0.018	0.035±0.019
C8:1-DC	0.027±0.016	0.042±0.009	0.032±0.012	0.040±0.011	0.044±0.014	0.024±0.009*
C10-OH/C8-DC	0.148±0.033	0.130±0.049	0.134±0.029	0.251±0.096*	0.183±0.091	0.080±0.007*
C12:2	0.043±0.023	0.038±0.015	0.028±0.013	0.031±0.010	0.033±0.013	0.023±0.005
C12:1	0.223±0.017	0.205±0.065	0.228±0.037	0.332±0.098	0.174±0.053	0.105±0.013*
C12	0.272±0.058	0.242±0.073	0.503±0.192	0.692±0.257	0.337±0.132	0.183±0.067*
C12:2-OH/C10:2-DC	0.168±0.071	0.116±0.017*	0.144±0.025	0.121±0.031	0.094±0.033	0.055±0.004*
C12:1-OH/C10:1-DC	0.120±0.029	0.128±0.044	0.120±0.020	0.212±0.081*	0.107±0.021	0.069±0.014*
C12-OH/C10-DC	0.113±0.048	0.105±0.036	0.151±0.023	0.301±0.121*	0.220±0.112	0.106±0.034*
C14:3	0.029±0.010	0.017±0.010	0.029±0.007	0.024±0.013	0.031±0.011	0.019±0.006
C14:2	0.338±0.102	0.247±0.063	0.401±0.103	0.425±0.091	0.208±0.056	0.133±0.053*
C14:1	0.588±0.125	0.583±0.276	1.025±0.209	1.407±0.400	0.782±0.257	0.442±0.155*
C14	0.762±0.182	0.778±0.316	1.632±0.516	2.465±0.894	1.014±0.324	0.594±0.279
C14:3-OH/C12:3-DC	0.013±0.004	0.017±0.009	0.012±0.008	0.013±0.014	0.016±0.011	0.011±0.007
C14:2-OH/C12:2-DC	0.144±0.052	0.139±0.055	0.139±0.028	0.240±0.079*	0.130±0.058	0.074±0.024
C14:1-OH/C12:1-DC	0.229±0.036	0.273±0.110	0.338±0.065	0.670±0.230*	0.380±0.119	0.172±0.051*
C14-OH/C12-DC	0.219±0.039	0.222±0.114	0.401±0.071	0.793±0.286*	0.532±0.230	0.193±0.054*
C16:3	0.077±0.017	0.075±0.037	0.113±0.022	0.183±0.048*	0.074±0.032	0.038±0.012
C16:2	0.508±0.108	0.490±0.274	1.052±0.284	1.688±0.375*	0.455±0.186	0.213±0.092*
C16:1	0.684±0.156	0.802±0.433	1.640±0.479	2.743±0.582*	1.117±0.476	0.584±0.258*
C16	2.373±0.745	2.639±1.131	5.590±2.191	8.142±2.650	2.540±0.818	1.656±1.145
C16:3-OH/C14:3-DC	0.021±0.006	0.020±0.011	0.027±0.008	0.048±0.014*	0.022±0.011	0.015±0.003
C16:2-OH/C14:2-DC	0.190±0.048	0.210±0.080	0.302±0.065	0.512±0.142*	0.220±0.084	0.096±0.031*
C16:1-OH/C14:1-DC	0.222±0.041	0.300±0.136	0.465±0.136	0.909±0.265*	0.441±0.195	0.189±0.068*
C16-OH/C14-DC	0.426±0.091	0.552±0.312	0.977±0.333	1.960±0.494*	0.930±0.531	0.310±0.130*
C18:3	0.487±0.077	0.629±0.358	1.067±0.301	1.572±0.231*	0.438±0.159	0.199±0.120*
C18:2	2.768±0.822	3.757±2.426	7.187±2.752	12.196±2.736*	2.098±0.900	1.249±1.152
C18:1	2.484±0.721	3.232±1.970	6.400±2.280	10.956±2.800*	2.603±0.924	1.702±1.353
C18	1.052±0.239	1.000±0.463	2.233±1.014	3.055±1.134	0.841±0.218	0.597±0.356
C18:3-OH/C16:3-DC	0.093±0.023	0.104±0.043	0.140±0.030	0.258±0.078*	0.096±0.044	0.036±0.008*
C18:2-OH/C16:2-DC	0.620±0.102	1.052±0.749	1.464±0.445	3.353±0.835*	0.761±0.402	0.276±0.127*
C18:1-OH/C16:1-DC	0.556±0.140	0.898±0.641	1.343±0.417	3.015±0.627*	1.056±0.547	0.370±0.148*
C18-OH/C16-DC	0.184±0.047	0.195±0.085	0.338±0.083	0.638±0.156*	0.254±0.108	0.120±0.065*
C20:4	0.269±0.060	0.220±0.090	0.352±0.047	0.354±0.117	0.201±0.060	0.090±0.118
C20:3	0.094±0.020	0.102±0.047	0.156±0.030	0.233±0.071*	0.057±0.022	0.061±0.045
C20:2	0.093±0.020	0.099±0.063	0.217±0.055	0.469±0.078*	0.075±0.024	0.062±0.051
C20:1	0.151±0.027	0.137±0.083	0.331±0.134	0.634±0.139*	0.095±0.055	0.086±0.067
C20	0.066±0.018	0.082±0.036	0.132±0.029	0.211±0.050*	0.054±0.014	0.037±0.024
C20:3-OH/C18:3-DC	0.045±0.013	0.045±0.009	0.048±0.007	0.066±0.023	0.039±0.025	0.019±0.014
C20:2-OH/C18:2-DC	0.073±0.019	0.082±0.028	0.098±0.018	0.223±0.079*	0.070±0.044	0.062±0.017
C20:1-OH/C18:1-DC	0.038±0.014	0.045±0.030	0.078±0.037	0.166±0.063*	0.047±0.016	0.025±0.006*
C20-OH/C18-DC/C22:6	0.077±0.019	0.061±0.027	0.109±0.023	0.082±0.042	0.028±0.018	0.012±0.014
C22:5	0.038±0.014	0.032±0.022	0.049±0.024	0.039±0.030	0.015±0.010	0.025±0.023
C22:4	0.016±0.009	0.022±0.013	0.029±0.011	0.016±0.011	0.018±0.009	0.011±0.012
C22:3	0.006±0.005	0.005±0.004	0.007±0.005	0.009±0.009	0.010±0.010	0.007±0.004
C22:2	0.014±0.006	0.010±0.006	0.010±0.004	0.016±0.008	0.008±0.003	0.008±0.007
C22:1	0.044±0.007	0.047±0.013	0.046±0.021	0.052±0.008	0.043±0.013	0.031±0.007
C22	0.024±0.008	0.030±0.015	0.022±0.009	0.031±0.019	0.023±0.010	0.012±0.004*

Metabolites	Sham-CH (n=6)	CH (n=6)	Sham-HF (n=6)	HF (n=6)	Sed (n=6)	PH (Run) (n=6)
Organic Acid						
lactate	3380.2±314.5	3789.5±1032.9	4459.8±383.9	6975.6±2021.1*	5955.1±786.4	4558.7±544.6*
succinate	362.5±12.6	340.8±48.6	447.3±33.1	538.2±72.5*	472.4±31.4	319.1±31.0*
malate	1007.5±92.9	858.4±110.4	1030.6±62.8	752.7±85.6*	726.6±125.6	462.2±39.7*
citrate	422.5±26.3	386.1±40.3	375.3±28.3	312.8±55.9	371.6±48.8	343.9±33.2
pyruvate	20.7±2.3	22.1±3.5	23.5±2.8	22.1±3.4	20.0±2.4	20.1±3.1
fumarate	125.5±12.7	104.0±12.0*	133.4±9.6	97.4±10.7*	109.7±12.8	66.8±5.5*
a-KG	10.2±1.0	10.0±1.7	10.6±2.1	7.8±1.0*	7.6±1.1	7.0±0.9
Lactate/Pyruvate	164.9±24.2	172.8±44.9	190.5±12.1	324.7±122.0*	300.2±36.2	227.8±16.4*
Amino Acid						
Glx	7493.8±812.1	6603.5±639.1*	6621.1±708.5	6156.5±582.7	9632.9±995.6	9486.3±945.4
Gly	657.0±52.7	668.8±101.4	625.5±56.9	676.9±62.9	563.3±67.7	570.0±60.3
Ala	1917.2±196.4	2072.6±133.1	2061.4±124.5	2166.5±241.1	1650.9±119.2	1382.3±70.9*
Ser	1301.8±133.2	1533.6±135.2*	1201.4±121.9	1714.8±73.7*	938.7±77.5	979.1±67.7
Leu/Ile	510.9±66.0	427.8±30.6*	463.1±49.7	510.5±56.7	327.5±16.5	293.2±18.7*
Asx	1594.9±183.9	1612.3±184.6	1538.8±170.1	1994.8±287.2*	2154.7±356.0	1616.7±217.4*
Pro	98.6±8.0	133.7±28.0*	103.6±7.2	146.8±15.3*	68.0±9.6	72.7±4.3
Val	429.3±37.8	348.3±47.3*	353.3±34.3	411.2±66.6	201.0±20.2	214.3±29.7
Met	79.4±4.6	92.2±9.4*	77.2±8.9	97.1±6.1*	77.5±8.7	80.2±11.7
His	331.0±50.4	211.8±16.1*	295.6±40.4	250.7±39.6	242.1±31.1	242.8±26.9
Phe	80.3±8.7	89.1±11.9	81.2±7.6	104.8±7.1*	57.7±5.6	58.6±5.2
Tyr	97.5±24.8	104.2±13.7	89.5±12.7	102.4±10.1	61.4±8.6	72.8±11.4
Orn	36.1±3.8	41.8±5.3	53.5±17.2	45.5±6.9	31.4±3.9	34.0±3.4
Cit	293.5±50.9	264.4±36.3	288.8±27.5	264.9±30.5	207.0±16.7	207.6±21.4
Arg	298.4±31.6	257.4±14.5*	306.2±20.9	287.5±23.5	235.7±10.0	266.8±15.5*

*$p < 0.05$ compared to corresponding controls.

Supplemental Table 8: Metabolite measurements from CH and HF plasma.

Metabolites	Sham-CH (n=5)	CH (n=6)	Sham-HF (n=7)	HF (n=6)
Acylcarnitine				
P-C0	30.5±6.7	31.6±5.6	30.3±5.8	30.2±4.9
P-C2	17.4±4.7	19.2±3.5	16.3±4.0	14.4±2.3
P-C3	0.36±0.05	0.31±0.06	0.30±0.06	0.20±0.04*
P-C4/Ci4	0.40±0.17	0.33±0.10	0.86±0.40	0.76±0.36
P-C5:1	0.30±0.06	0.31±0.07	0.36±0.09	0.30±0.05
P-C5	0.112±0.021	0.124±0.066	0.147±0.063	0.124±0.046
P-C4-OH	0.157±0.060	0.213±0.061	0.162±0.029	0.116±0.029*
P-C6	0.113±0.031	0.104±0.033	0.105±0.045	0.097±0.024
P-C5-OH	0.084±0.019	0.089±0.017	0.081±0.022	0.058±0.011*
P-C3-DC	0.030±0.014	0.022±0.008	0.019±0.008	0.011±0.006
P-C4-DC/Ci4-DC	0.026±0.018	0.044±0.009	0.029±0.030	0.020±0.018
P-C8:1	0.023±0.009	0.027±0.010	0.021±0.008	0.021±0.008
P-C8	0.209±0.177	0.205±0.091	0.142±0.096	0.133±0.076
P-C5-DC	0.013±0.018	0.018±0.022	0.007±0.018	0.002±0.006
P-C8:1-OH/C6:1-DC	0.217±0.090	0.174±0.123	0.129±0.043	0.065±0.061
P-C6-DC	0.039±0.006	0.023±0.013*	0.038±0.013	0.015±0.011*
P-C10:3	0.035±0.010	0.037±0.014	0.031±0.018	0.024±0.009
P-C10:2	0.008±0.005	0.016±0.009	0.017±0.010	0.010±0.010
P-C10:1	0.027±0.016	0.032±0.009	0.026±0.006	0.031±0.014
P-C10	0.027±0.020	0.027±0.017	0.027±0.016	0.031±0.017
P-C7-DC	0.009±0.007	0.017±0.011	0.012±0.007	0.020±0.015
P-C8:1-DC	0.060±0.016	0.064±0.023	0.048±0.007	0.046±0.021
P-C10-OH/C8-DC	0.014±0.031	0.252±0.258	0.027±0.072	0.071±0.112
P-C12:1	0.042±0.026	0.038±0.030	0.037±0.010	0.049±0.014
P-C12	0.082±0.012	0.085±0.011	0.075±0.013	0.076±0.014
P-C12-OH/C10-DC	0.007±0.006	0.012±0.010	0.005±0.007	0.006±0.006
P-C14:2	0.046±0.040	0.035±0.022	0.037±0.037	0.034±0.026
P-C14:1	0.060±0.019	0.068±0.017	0.063±0.016	0.065±0.011
P-C14	0.053±0.012	0.063±0.021	0.066±0.017	0.060±0.012
P-C14:1-OH	0.016±0.010	0.025±0.006	0.017±0.004	0.020±0.004
P-C14-OH/C12-DC	0.009±0.004	0.013±0.005	0.010±0.003	0.010±0.001
P-C16:2	0.021±0.009	0.024±0.005	0.021±0.010	0.020±0.005
P-C16:1	0.052±0.008	0.057±0.019	0.050±0.013	0.054±0.008
P-C16	0.126±0.031	0.132±0.037	0.153±0.020	0.144±0.041
P-C16:1-OH/C14:1-DC	0.017±0.007	0.023±0.005	0.013±0.003	0.017±0.005
P-C16-OH/C14-DC	0.010±0.003	0.011±0.003	0.014±0.005	0.011±0.004
P-C18:2	0.081±0.012	0.088±0.019	0.075±0.011	0.079±0.017
P-C18:1	0.164±0.034	0.182±0.051	0.162±0.017	0.166±0.046
P-C18	0.034±0.007	0.036±0.011	0.043±0.010	0.038±0.010
P-C18:2-OH	0.010±0.004	0.016±0.005*	0.009±0.006	0.011±0.002
P-C18:1-OH/C16:1-DC	0.027±0.010	0.029±0.005	0.022±0.003	0.026±0.003*
P-C18-OH/C16-DC	0.008±0.017	0.037±0.061	0.027±0.047	0.014±0.035
P-C20:4	0.029±0.009	0.028±0.007	0.031±0.007	0.032±0.006
P-C20	0.004±0.001	0.004±0.001	0.006±0.002	0.004±0.002
P-C22	0.003±0.002	0.004±0.001	0.005±0.001	0.003±0.002
Amino Acid				
P-Glx	50.3±9.7	50.1±7.6	53.9±5.7	54.3±6.5
P-Gly	267.8±61.4	236.4±47.0	220.2±52.8	232.2±28.4
P-Ala	396.8±85.8	352.8±91.4	332.1±29.5	349.7±57.6
P-Ser	114.3±14.4	105.7±14.0	99.6±18.2	104.9±18.5
P-Leu/Ile	117.0±21.0	111.3±23.6	108.3±17.9	157.4±21.4*
P-Asx	127.9±69.4	157.8±46.9	131.0±70.4	92.3±39.3
P-Pro	59.6±11.3	56.7±11.0	49.5±4.9	55.6±7.9
P-Val	118.5±14.8	113.5±22.4	117.5±18.5	133.2±15.6
P-Met	47.8±6.3	50.7±6.4	40.0±3.6	45.2±4.7*
P-His	17.7±6.6	18.7±2.5	19.2±4.1	23.4±3.9
P-Phe	52.4±4.3	55.4±8.9	50.2±5.2	64.6±5.4*
P-Tyr	68.9±7.8	67.6±12.5	61.1±9.9	65.4±8.8
P-Orn	42.3±5.8	39.5±9.2	31.9±4.3	38.4±6.3
P-Cit	54.5±12.9	54.9±10.5	43.5±7.9	60.4±11.7*
P-Arg	93.4±19.6	87.7±18.0	86.4±10.5	90.5±14.9

*$p < 0.05$ compared to sham control.

Supplemental Table 9. Cardiac hypertrophy in PH model.

Parameters	Sedentary	PH (Run)	p-value
N	15	15	
Body weight (g)	20.84 ± 1.50	21.67 ± 1.14	0.09
Bi-ventricle weight (g)	0.0889 ± 0.0102	0.1019 ± 0.0057*	<0.001
Bi-ventricle w/BW	4.26 ± 0.29	4.71 ± 0.33*	<0.001

*$p < 0.05$ compared to sedentary control. w/BW, weight/body weight ratio; g, grams

Supplemental Table 10. Differentially expressed genes in PH myocardium.

Probe ID	Symbol	Gene Name	PH (Run)	
			FC	DE
10359867	Lrrc52	leucine rich repeat containing 52	-1.553	**1.000**
10476793	NA	NA	-1.351	**0.994**
10476791	NA	NA	-1.443	**0.989**
10472426	Xirp2	xin actin-binding repeat containing 2	1.539	**0.988**
10488108	Esf1	ESF1, nucleolar pre-rRNA processing protein, homolog (S. cerevisiae)	1.513	**0.986**
10452516	Ankrd12	ankyrin repeat domain 12	1.378	**0.981**

FC, fold change; DE, posterior probability of differential expression; genes with DE ≥ 0.950 (bolded) are significantly regulated.

Supplemental Figure 1

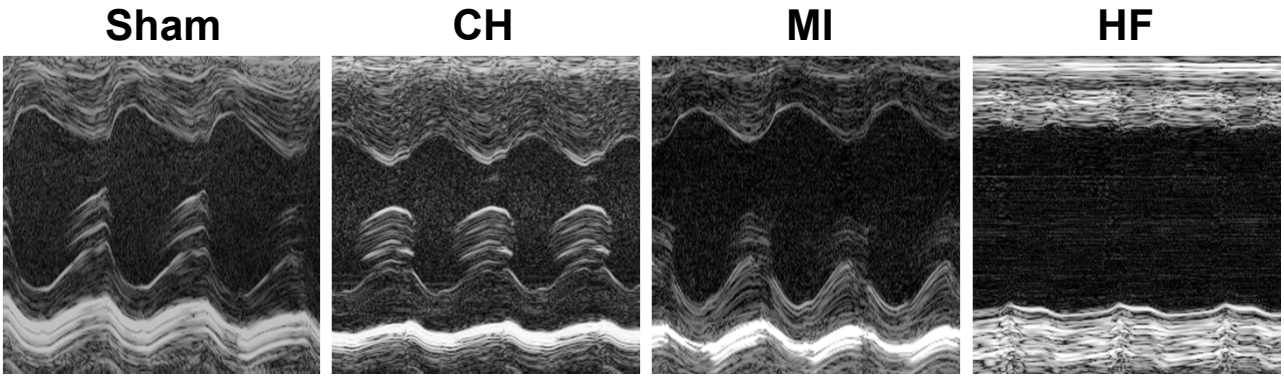

Supplemental Figure 2

A.

TCA

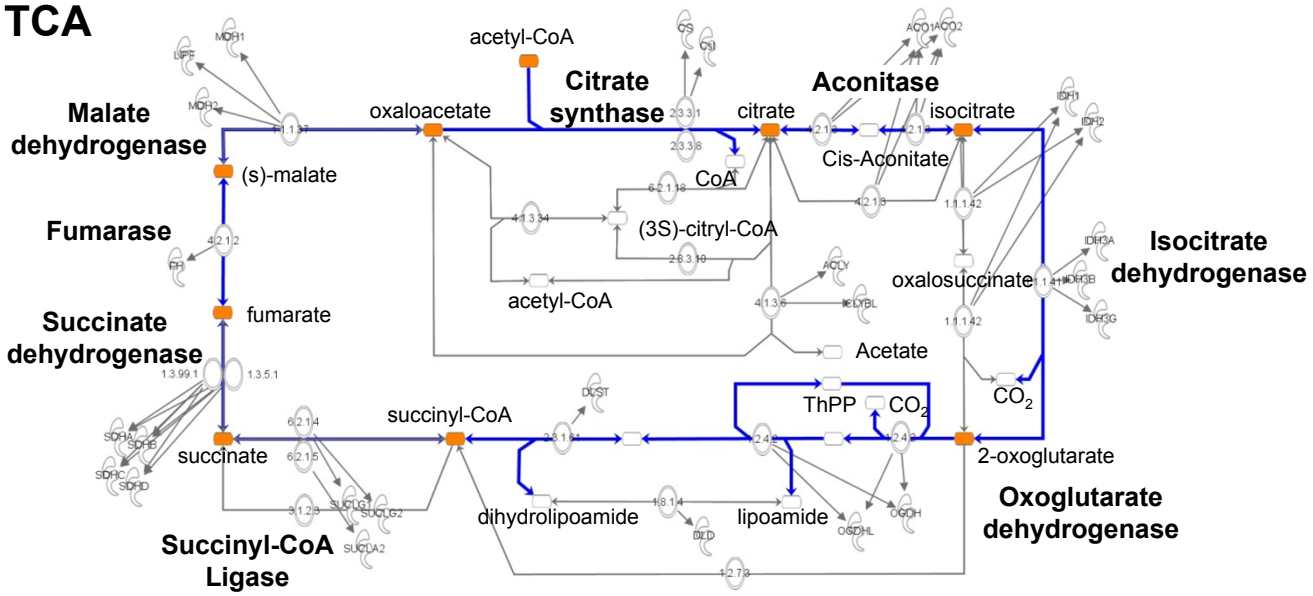

B.

ETC/OXPHOS

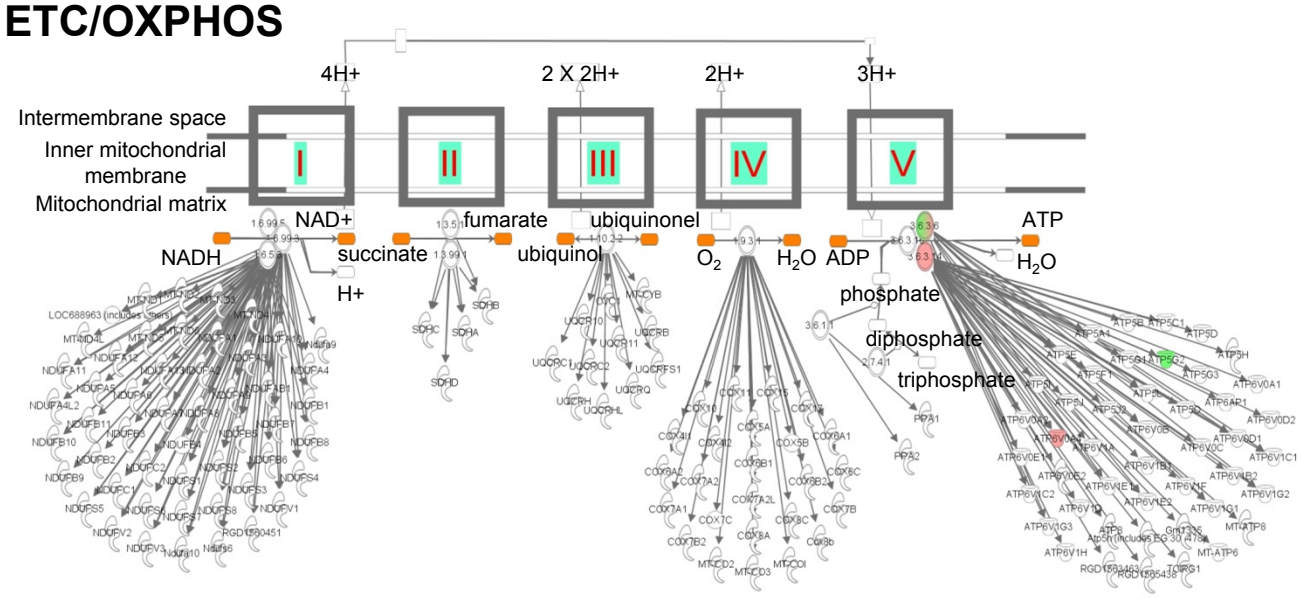

Supplemental Figure 3

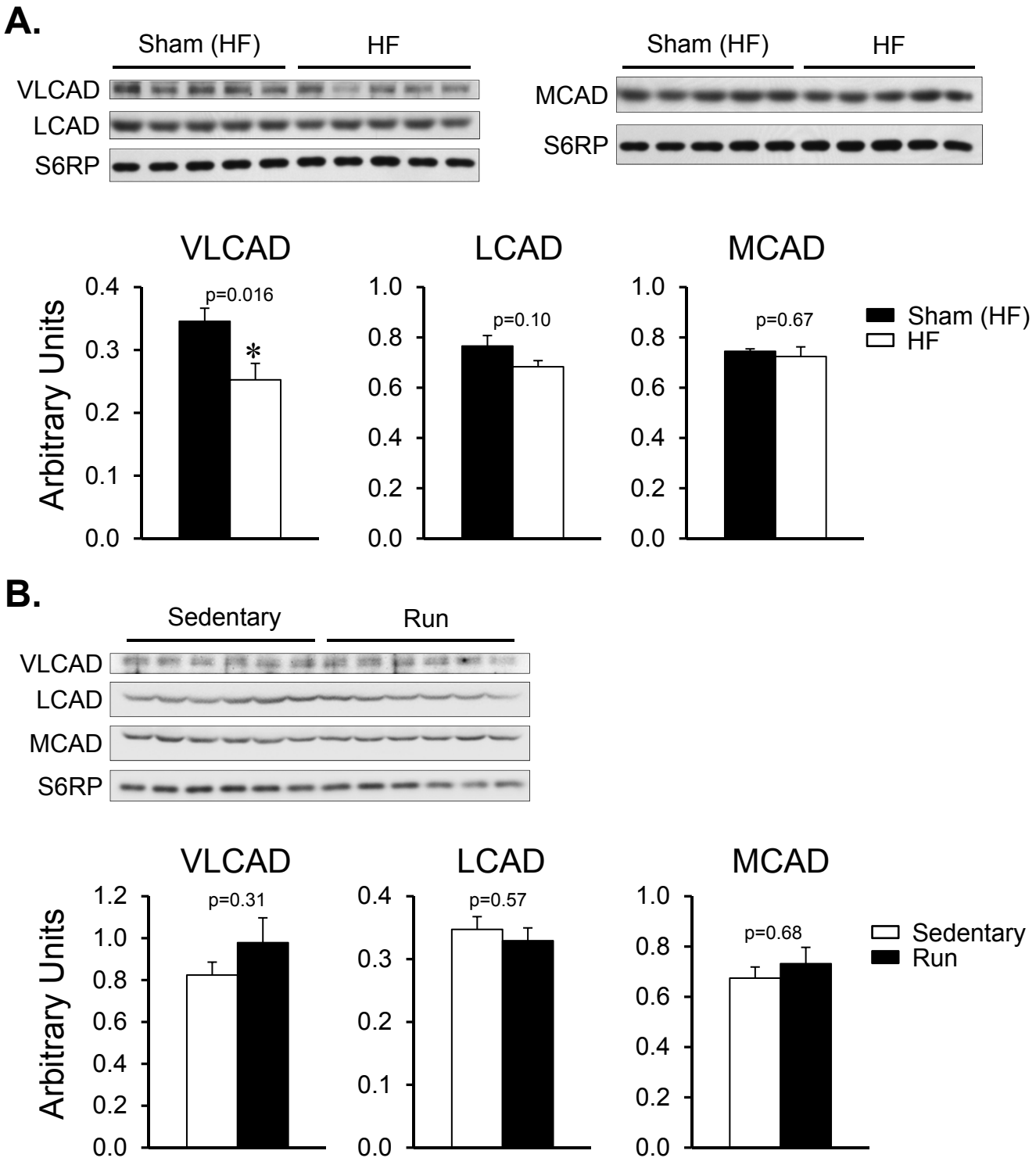

SUPPLEMENTAL FIGURE LEGENDS

Figure 1. Representative ventricular remodeling in compensated (CH) and decompensated (HF) pressure overload cardiac hypertrophy models. (A) Representative M-mode echocardiographic images through the mid-LV from 12-week-old female C57BL6/J mice one month after being subjected to sham, transverse aortic constriction (CH), small apical myocardial infarction (MI), or combined transverse aortic constriction with small myocardial infarction (HF).

Figure 2. Minimal changes in expression of myocardial genes involved in tricarboxylic acid (TCA) cycle, electron transport chain (ETC)/oxidative phosphorylation (OXPHOS) in HF. Pathway map showing genes significantly (DE ≥ 0.950) upregulated (pink) or downregulated (green) in HF compared to sham control in canonical pathways such as (A) TCA and (B) ETC/OXPHOS identified by Ingenuity Pathway Analysis. Complexes I through V in the ETC/OXPHOS pathway are denoted as I, II, III, IV, and V. The ovals in the map represent enzyme complexes.

Figure 3. Determination of fatty acid β-oxidation (FAO) protein levels in HF samples. Representative Western blots assessing levels of protein extracted from hearts of (A) HF and corresponding sham-operated controls and (B) sedentary and wheel-exercised mice (Run) for the following proteins: acyl-Coenzyme A dehydrogenase, very long chain (VLCAD), acyl-Coenzyme A dehydrogenase, long-chain (LCAD) and medium chain (MCAD). Ribosomal protein S6 (S6RP) was used as loading control. Quantification of the blot analysis is shown at the bottom of each panel. Bars represent mean±S.E. *$p < 0.05$ compared with corresponding control

(n=5-6 per group).

SUPPLEMENTAL REFERENCES

1. Lai L, Wang M, Martin OJ, Leone TC, Vega RB, Han X, Kelly DP. A role for peroxisome proliferator-activated receptor gamma coactivator 1 (PGC-1) in the regulation of cardiac mitochondrial phospholipid biosynthesis. *J Biol Chem*. 2014;289:2250-2259.

2. Huss JM, Imahashi K, Dufour CR, Weinheimer CJ, Courtois M, Kovacs A, Giguere V, Murphy E, Kelly DP. The nuclear receptor ERRalpha is required for the bioenergetic and functional adaptation to cardiac pressure overload. *Cell Metab*. 2007;6:25-37.

3. Lai L, Leone TC, Zechner C, Schaeffer PJ, Kelly SM, Flanagan DP, Medeiros DM, Kovacs A, Kelly DP. Transcriptional coactivators PGC-1alpha and PGC-lbeta control overlapping programs required for perinatal maturation of the heart. *Genes Dev*. 2008;22:1948-1961.

4. Martin OJ, Lai L, Soundarapandian MM, Leone TC, Zorzano A, Keller MP, Attie AD, Muoio DM, Kelly DP. A role for peroxisome proliferator-activated receptor gamma coactivator-1 in the control of mitochondrial dynamics during postnatal cardiac growth. *Circ Res*. 2014;114:626-636.

5. Allen DL, Harrison BC, Maass A, Bell ML, Byrnes WC, Leinwand LA. Cardiac and skeletal muscle adaptations to voluntary wheel running in the mouse. *J Appl Physiol*. 2001;90:1900-1908.

6. Huss JM, Torra IP, Staels B, Giguere V, Kelly DP. Estrogen-related receptor alpha directs peroxisome proliferator-activated receptor alpha signaling in the transcriptional control of energy metabolism in cardiac and skeletal muscle. *Mol Cell Biol*. 2004;24:9079-9091.

7. Cresci S, Wright LD, Spratt JA, Briggs FN, Kelly DP. Activation of a novel metabolic gene regulatory pathway by chronic stimulation of skeletal muscle. *Am J Physiol*. 1996;270:C1413-1420.

8. Kelly DP, Kim JJ, Billadello JJ, Hainline BE, Chu TW, Strauss AW. Nucleotide sequence of medium-chain acyl-CoA dehydrogenase mRNA and its expression in enzyme-deficient human tissue. *Proc Natl Acad Sci U S A*. 1987;84:4068-4072.

9. Hainline BE, Kahlenbeck DJ, Grant J, Strauss AW. Tissue specific and developmental expression of rat long-and medium-chain acyl-CoA dehydrogenases. *Biochim Biophys Acta*. 1993;1216:460-468.

10. Exil VJ, Roberts RL, Sims H, McLaughlin JE, Malkin RA, Gardner CD, Ni G, Rottman JN, Strauss AW. Very-long-chain acyl-coenzyme a dehydrogenase deficiency in mice. *Circ Res*. 2003;93:448-455.

11. Saks VA, Veksler VI, Kuznetsov AV, Kay L, Sikk P, Tiivel T, Tranqui L, Olivares J, Winkler K, Wiedemann F, Kunz WS. Permeabilized cell and skinned fiber techniques in studies of mitochondrial function in vivo. *Mol Cell Biochem*. 1998;184:81-100.

12. Irizarry RA, Hobbs B, Collin F, Beazer-Barclay YD, Antonellis KJ, Scherf U, Speed TP. Exploration, normalization, and summaries of high density oligonucleotide array probe level data. *Biostatistics*. 2003;4:249-264.

13. Newton MA, Kendziorski CM, Richmond CS, Blattner FR, Tsui KW. On differential variability of expression ratios: improving statistical inference about gene expression changes from microarray data. *J Comput Biol*. 2001;8:37-52.

14. Kendziorski CM, Newton MA, Lan H, Gould MN. On parametric empirical Bayes methods for comparing multiple groups using replicated gene expression profiles. *Stat Med*. 2003;22:3899-3914.

15. Millington DS, Kodo N, Norwood DL, Roe CR. Tandem mass spectrometry: a new method for acylcarnitine profiling with potential for neonatal screening for inborn errors of metabolism. *J Inherit Metab Dis*. 1990;13:321-324.

16. An J, Muoio DM, Shiota M, Fujimoto Y, Cline GW, Shulman GI, Koves TR, Stevens R, Millington D, Newgard CB. Hepatic expression of malonyl-CoA decarboxylase reverses muscle, liver and whole-animal insulin resistance. *Nat Med*. 2004;10:268-274.

17. Wu JY, Kao HJ, Li SC, Stevens R, Hillman S, Millington D, Chen YT. ENU mutagenesis identifies mice with mitochondrial branched-chain aminotransferase deficiency resembling human maple syrup urine disease. *J Clin Invest*. 2004;113:434-440.

18. Jensen MV, Joseph JW, Ilkayeva O, Burgess S, Lu D, Ronnebaum SM, Odegaard M, Becker TC, Sherry AD, Newgard CB. Compensatory responses to pyruvate carboxylase suppression in islet beta-cells. Preservation of glucose-stimulated insulin secretion. *J Biol Chem*. 2006;281:22342-22351.